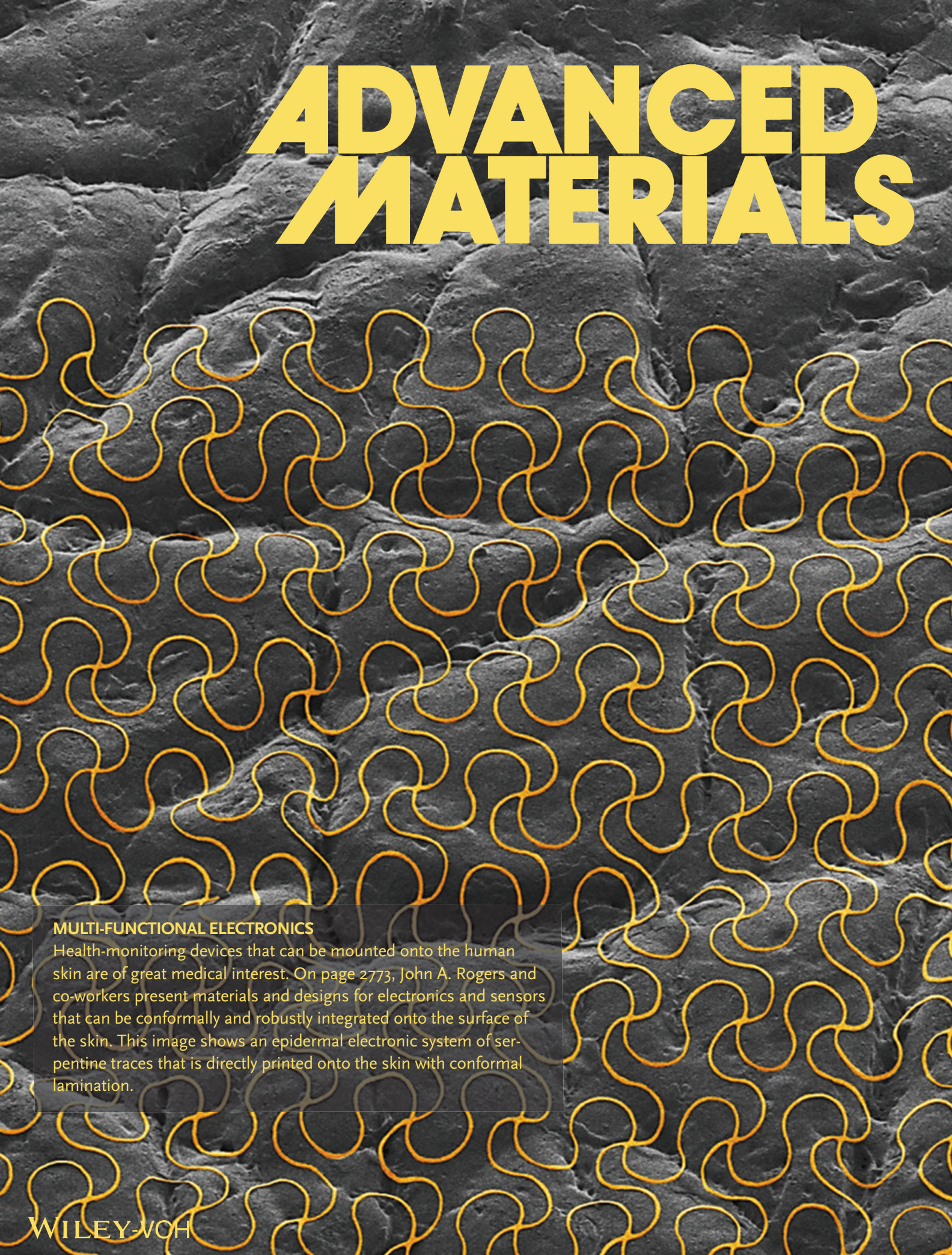


ADVANCED MATERIALS

A scanning electron micrograph (SEM) of human skin, showing its characteristic wrinkled and textured surface. Overlaid on this skin surface is a dense, repeating pattern of bright yellow, serpentine traces. These traces form a grid of interconnected, rounded, loop-like shapes that conform to the underlying skin topography. The background skin is in grayscale, providing a high-contrast backdrop for the yellow traces.

MULTI-FUNCTIONAL ELECTRONICS

Health-monitoring devices that can be mounted onto the human skin are of great medical interest. On page 2773, John A. Rogers and co-workers present materials and designs for electronics and sensors that can be conformally and robustly integrated onto the surface of the skin. This image shows an epidermal electronic system of serpentine traces that is directly printed onto the skin with conformal lamination.

Multifunctional Epidermal Electronics Printed Directly Onto the Skin

Woon-Hong Yeo, Yun-Soung Kim, Jongwoo Lee, Abid Ameen, Luke Shi, Ming Li, Shuodao Wang, Rui Ma, Sung Hun Jin, Zhan Kang, Yonggang Huang, and John A. Rogers*

Health and wellness monitoring devices that mount on the human skin are of great historical and continuing interest in clinical health care, due to their versatile capabilities in non-invasive, physiological diagnostics.^[1–4] Conventional technologies for this purpose typically involve small numbers of point contact, flat electrode pads that affix to the skin with adhesive tapes and often use conductive gels to minimize contact impedances.^[5] This type of approach, as well as related ones that eliminate the gel, have strong clinical utility but limited value in everyday life due to discomfort and loss of adhesion that arise from the unfavorable nature of the skin/electrode interface.^[4,6] Recent work^[7] demonstrates an alternative strategy, based on fully integrated electronics that have soft, stretchable forms designed to match the physical properties (modulus, thickness, and areal mass density) of the epidermis itself. Such devices, which we refer to as epidermal electronic systems (EES), laminate and adhere directly on the skin, in a conformal manner, via the action of van der Waals forces alone. The result is a natural interface that is capable of accommodating the motions

of the skin without any mechanical constraints, thereby establishing not only a robust, non-irritating skin/electrode contact but also the basis for intimate integration of diverse classes of electronic and sensor technologies directly with the body. The present work extends these ideas through the development of significantly thinner (by 20–30 times) variants of EES and of materials that facilitate their robust bonding to the skin, in ways that allow continuous integration through all aspects of daily life including exercise and bathing. Demonstrations in a multifunctional EES capable of measuring electrophysiological (EP) signals, such as electrocardiograms (ECG) and electromyograms (EMG), as well as temperature and mechanical strain illustrate the materials, mechanics and mounting schemes.

Figure 1a shows a representative multifunctional EES of this type. The construct consists of an interconnected collection of thin, filamentary serpentine (FS) conductive traces and integrated devices, all in an open mesh layout. Such designs provide extremely low effective elastic moduli and large deformability, at the level of the overall system, even when the mesh incorporates brittle, high modulus materials such as silicon.^[7] These properties allow the EES to follow the contoured surfaces and time-dynamic motions of the skin, in a natural way. The EP sensor includes three electrodes, each in the form of an FS mesh with exposed metal (Au) that contacts the skin directly, for measurement (MEA), ground (GND) and reference (REF). The sensors for strain and temperature use silicon nanomembranes (Si NMs; thickness: 260 nm, width: 30 μm , length: 500 μm) and platinum meander lines (Pt; thickness: 40 nm, width: 100 μm), respectively. The layout involves top and bottom layers of polyimide (PI; 0.3 μm in thickness, Sigma-Aldrich, USA) that place the active sensing components and interconnect wiring at the neutral mechanical plane (NMP). This design minimizes bending-induced strains in the critical materials. The exceptions to this NMP configuration are at the EP sensor electrodes and at the contact pads for external data acquisition, both of which require metal on exposed surfaces. The completed device (Figure 1a) has a total thickness of 0.8 μm in its thickest region. By point of comparison, this thickness is more than fifty times smaller than the thinnest area of the human epidermis (typical thickness: 50 μm to 1.5 mm)^[8] and is, in fact, more than ten times smaller than the thickness of an individual keratinocyte (typical diameter: 11 μm).^[9]

The fabrication follows procedures described in the Experimental Section, in which all processing is performed on a silicon wafer. A double transfer process involving a water soluble tape (3M, USA) releases the resulting device from the wafer

Dr. W.-H. Yeo, Y.-S. Kim, J. Lee, A. Ameen,
L. Shi, Dr. S. Wang, Dr. S. H. Jin
Department of Materials Science and Engineering
Beckman Institute for Advanced Science and Technology
and Frederick Seitz Materials Research Laboratory
University of Illinois at Urbana-Champaign
Urbana, Illinois 61801, USA



Dr. M. Li, Prof. Z. Kang
State Key Laboratory of Structural Analysis for Industrial Equipment
Dalian University of Technology
Dalian, 116024, China

Dr. R. Ma
Department of Bioengineering
University of California
San Diego, La Jolla, California 92093, USA

Prof. Y. Huang
Department of Mechanical Engineering and
Department of Civil and Environmental Engineering
Northwestern University
Evanston, Illinois 60208, USA

Prof. J. A. Rogers
Department of Materials Science and Engineering
Beckman Institute for Advanced Science and Technology
and Frederick Seitz Materials Research Laboratory
University of Illinois at Urbana-Champaign
Urbana, Illinois 61801, USA
E-mail: jrogers@illinois.edu

DOI: 10.1002/adma.201204426

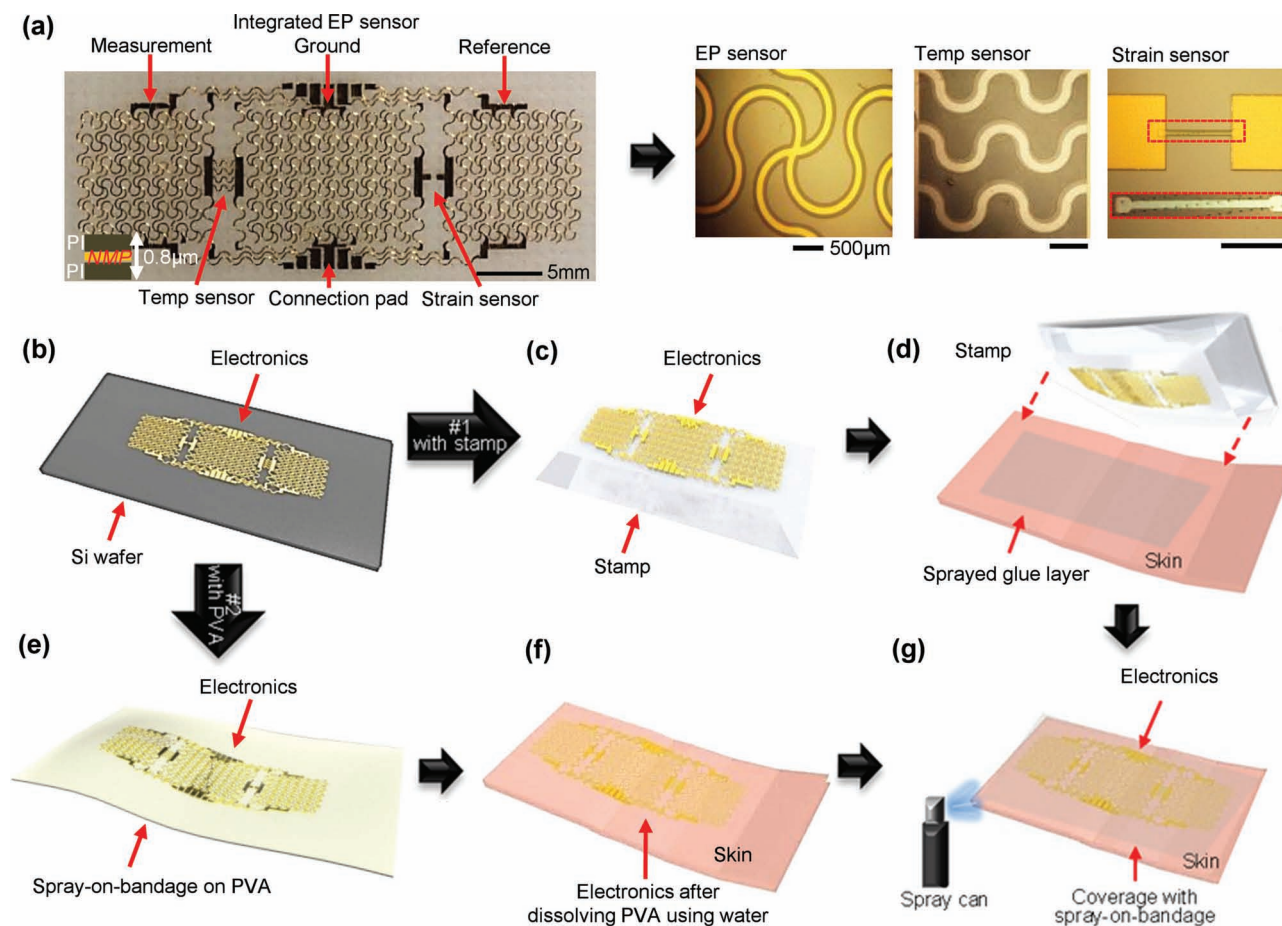


Figure 1. Multifunctional epidermal electronic systems (EES), in ultrathin formats, robustly bonded to and encapsulated on the skin. (a) Optical micrographs of a multifunctional EES (left) that includes an EP sensor constructed in an array of filamentary serpentine structures (magnified view, first frame on the right), a temperature sensor in a meander shape (middle frame on the right), and a mechanical strain sensor that uses a silicon nanomembrane resistor (rightmost frame). Scale bar is 500 μm . (b) Releasing the completed EES from the supporting wafer allows transfer either to an elastomeric stamp or to a sheet of polyvinylalcohol. (c) and (d) Transfer of the EES directly onto skin after application of a thin layer of a spray-on-bandage to facilitate adhesion. (e) and (f) Placement of the EES on the skin, followed by dissolution of the PVA in water, leaves the EES mounted on the skin. (g) Application of a layer of spray-on-bandage encapsulates the devices, ensures their strong bonding to the skin, and provides environmental and mechanical protection.

to allow integration on the skin (Figures 1c and 1e). Two procedures for this integration work particularly well. In the first approach (#1), the EES is placed on the surface of an elastomeric stamp and then transfer printed directly onto the skin. Here, a thin layer (~ 200 nm) of spray-on-bandage (Liquid bandage; 3 M Nexcare, USA) serves as an adhesive to facilitate transfer. The second (#2) involves transfer to a water soluble sheet of polyvinyl alcohol (PVA, Haining Sprutop Chemical Tech, China). Application of water washes this sheet away after mounting on the skin, to leave only the EES. In both cases, additional layers of spray-on-bandage can be applied directly on top of the EES and on adjacent regions of the skin (Figure 1g), to improve the robustness of integration. The steps for direct printing and subsequent encapsulation (Figures 1c, 1d and 1g) appear in Supporting Information (Movie S1).

The key feature of these strategies is that they do not require a separate substrate for the EES. The outcome is a reduction in device thickness by nearly 30 times compared to original EES

configurations, which use low modulus silicone membranes as substrates.^[7] This ultrathin geometry significantly reduces the flexural rigidity, and also improves the bendability and degree of conformal contact with the skin. High resolution scanning electron microscopy (SEM; S4800, Hitachi, USA) reveals these effects, as well as the role of geometry in the EES designs. These investigations used skin replicas prepared by first creating a silicone mold by casting a liquid precursor (Dragon skin; Smooth-On, USA) on the forearm and then curing it into a solid form. Casting and curing a prepolymer to polydimethylsiloxane (PDMS; Dow Corning, USA) yields a surface that replicates the skin. The mounting procedures of Figures 1c and 1d enable integration of EES onto these artificial surfaces.

Figure 2a corresponds to a skin replica before application of the adhesive layer of spray-on-bandage. The surface of the skin is characterized by structures with relief amplitudes between 15 and 100 μm and lateral dimensions between 40 and

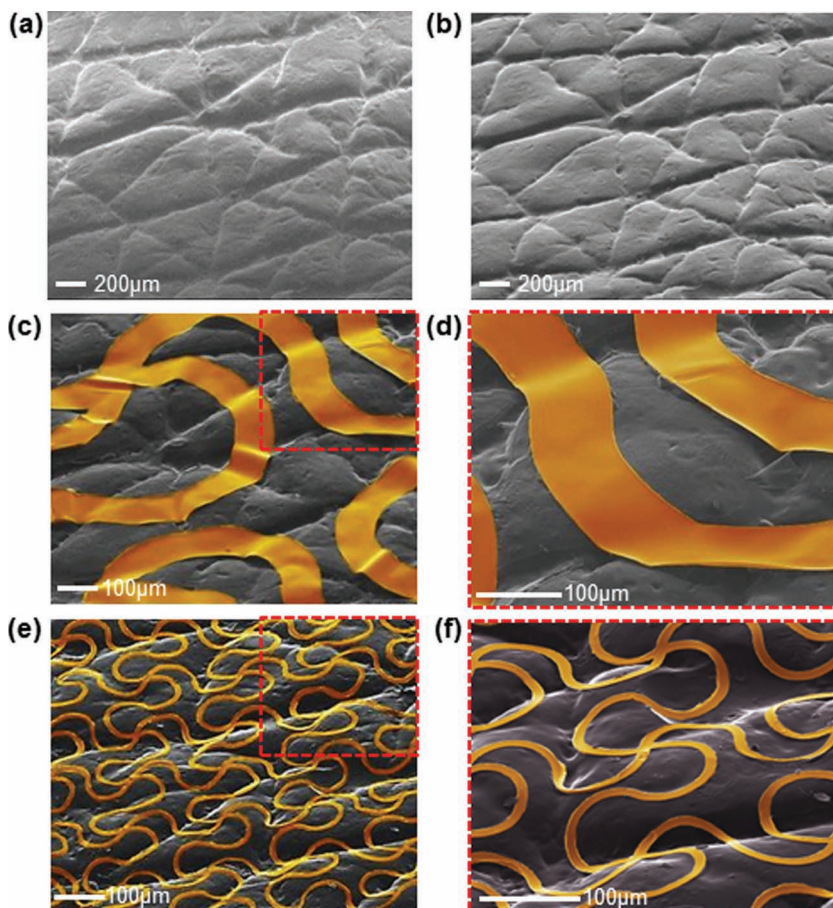


Figure 2. Relationship between EES design and degree of conformal contact with the skin. The studies use silicone surface replicas made by a two step process of casting and curing. (a) Image of a skin replica created from the forearm. (b) Skin replica after application of a ~ 200 nm thick layer of a spray-on-bandage. (c) Colorized SEM image of an EES that uses FS structures (gold) with widths of $100 \mu\text{m}$ mounted on the skin replica. (d) Magnified view of this image. (e) Colorized SEM image of an EES that uses FS structures (gold) with widths of $10 \mu\text{m}$ mounted on the skin replica. (f) Magnified view of this image.

$1000 \mu\text{m}$.^[10,11] The spray-on-bandage coating is conformal, and reduces some of this initial roughness (Figure 2b). The thicknesses of coatings used here are between 0.5 and $1 \mu\text{m}$, as evaluated on films deposited on microscope glass slides (Ted Pella, USA) using a combination of optical microscopy (Olympus, USA), atomic force microscopy (AFM; Asylum, USA), and surface profilometry (Dektak 3030, Veeco, USA) as shown in Figures S1a, S1b, and S1c, respectively. The EES layout that incorporates $100 \mu\text{m}$ wide FS traces follows most of the topography of the skin, but fails to penetrate into the deepest creases and pits (Figures 2c and 2d). The $100 \mu\text{m}$ -width is near the outer range of the sizes of relief features on the skin, as described earlier.^[10,11] Reducing the width by ten times, to $10 \mu\text{m}$, significantly improves the conformality, as shown in Figures 2e and 2f. This enhanced level of contact not only improves the mechanical robustness of integration, but it also facilitates electrical recording of EP signals through the skin, as described subsequently.

The layers of spray-on-bandage play critical roles. Of many varieties that were tested, two commercial materials worked

particularly well (Spray bandage, Walgreens; and Liquid bandage, 3M Nexcare, USA) due to their ease of use, adherence to the EES and ability to function in thin geometries. Their application involves spray deposition of a blend of an acrylate terpolymer and a polyphenylmethylsiloxane with hexamethylsiloxane as a volatile solvent. Upon evaporation, such formulations yield thin, solid conformal and transparent coatings on the skin and the EES. Modest variations in thickness across the coated area do not significantly change the performance of the EES. Theoretical mechanics modeling reveals the effects. The stretchability remains relatively constant for thicknesses from 1 to $5 \mu\text{m}$ (Figure S1d).

These films provide hydrophobic, waterproof surfaces (Figure S1e; contact angle with water $\sim 92.9^\circ$ evaluated by ImageJ, plug-in 'drop analysis'; National Institutes of Health, USA) that can block water, dirt and other debris, but offer sufficient levels of breathability to avoid adverse effects on the skin even during sweating (see the illustration in Figure S1e).^[12–15] Encapsulation of EES immediately after integration onto the skin typically involves three to four coatings of spray-on-bandage. These materials can also promote adhesion of EES to the skin and/or the PVA. Figure 3a (left) provides images of a representative EES integrated by direct printing on the forearm, and then encapsulation with spray-on-bandage. The images (center) illustrate responses to compression and extension of the skin induced by pinching. In all cases, the EES follows the natural deformations of the skin, without constraint. Fatigue tests, consisting of repeated cycles of pinching/releasing of the skin (cycle = 500; Figure S1f) demonstrate excellent robustness.

The spray-on-bandage materials have higher modulus ($\sim 85 \times 10^6$ Pa, Figure S1g) and lower elongation ($\sim 130\%$) than the silicone substrate polymers used previously (Ecoflex00-30; modulus: $\sim 69 \times 10^3$ Pa and elongation: 900% , Smooth-on, USA),^[7] but their thicknesses are nearly thirty times smaller (i.e., $\sim 1 \mu\text{m}$ compared to $30 \mu\text{m}$). The net effect is that the levels of deformability of EES integrated on the skin with these two classes of materials are qualitatively similar. Neither case showed any significant mechanical sensation of the presence of devices on the skin, irritation or discomfort.

An important aspect of the materials and mounting procedures presented here is that they yield levels of mechanical robustness and lifetime of wearability in real-world situations that exceed significantly those of our previously reported approaches.^[7] Demonstrations of these features involve mounting EES devices on the forearms of six volunteers (age: 21–32) and then evaluating them periodically, both visually and functionally, during a two week period. The results qualitatively

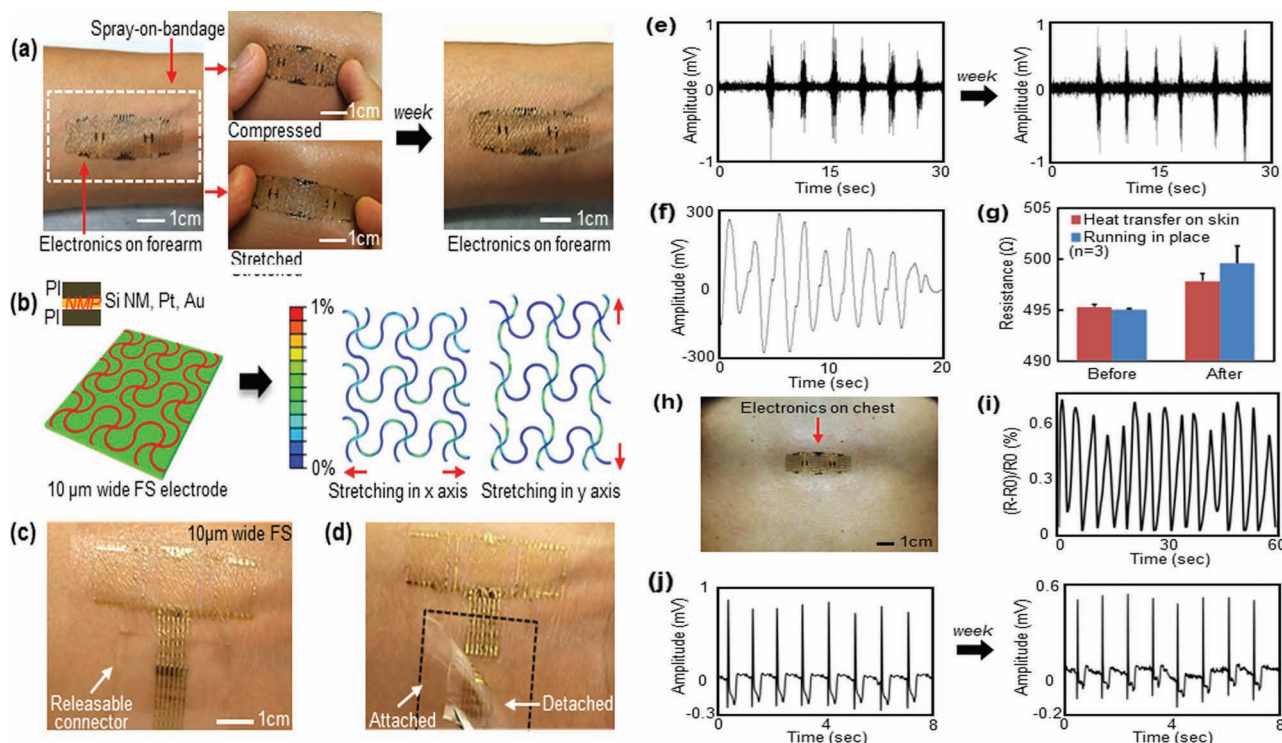


Figure 3. Applications of multifunctional EES for EP-, temperature-, and strain sensing on human skin. (a) EES mounted on the forearm and encapsulated with a layer of spray-on-bandage (left), under compression and extension of the skin (center), and after wearing for one week (right). (b) Finite element analysis of an EES comprised of a FS mesh with 10 μm widths, under mechanical stretching along the x and y directions. (c) EES on the skin with a releasable connector. (d) Detaching the releasable connector with a tweezer. (e) Demonstration of surface EMG recorded just after mounting a multifunctional EES on the forearm and after wearing for one week. (f) Recording of strain change upon bending the wrist inward and outward. (g) Change in resistance of a temperature sensor in a multifunctional EES upon heating with a hairdryer and after exercise (number of trials; $n = 3$ with standard deviation). (h) Image of a multifunctional EES mounted on the chest. (i) Time dependent strain measured during breathing using a device like that shown in (h). (j) ECG recorded using a device like that shown in (h).

indicate strong bonding, capable of accommodating motions, water and sweat during normal living behaviors, ranging from taking showers, to working, and exercising, for between one and two weeks. In demanding situations, a single application of spray-on-bandage ($<0.5 \mu\text{m}$ thick) applied once a day or once every other day affords the best results. Figure 3a (right) provides an image of an EES on the forearm after a week of use. A movie in the Supporting Information (Movie S2) shows a representative EES on the skin during physical abrasion, and washing with soap and water.

Eventual failure of the devices results from fracture and peeling in small pieces, likely due to exfoliation of dead cells from the surface of the skin, rather than premature loss of adhesion. Peel tests using a force gauge (Mark-10, USA) reveal quantitative values for the adhesion strength (Figure S1h). The examined materials include silicone membranes (Ecoflex; Smooth-On, USA) like used previously,^[7] a different formulation of this material (Solaris; Smooth-On, USA), spray-on bandages and conventional medical dressings, all with similar lateral dimensions ($\sim 9 \text{ cm}^2$ squares) applied to a region of the forearm without hair. 20 μm -thick silicone membranes show average adhesion forces of $0.24 \pm 0.02 \text{ N}$ (Ecoflex) and $0.37 \pm 0.01 \text{ N}$ (Solaris). By contrast, 1.1 μm -thick coatings of spray-on-bandage exhibit forces of $0.98 \pm 0.03 \text{ N}$, which approach

those observed in conventional medical dressings (Tegaderm, 3M Nexcare, USA), $1.02 \pm 0.01 \text{ N}$ ($\sim 35 \mu\text{m}$ in thickness).^[16] In fact, with procedures introduced here, such dressings themselves can serve as substrates and/or encapsulants for EES. These options can be attractive because they offer proven characteristics for long-term use both inside and outside of hospital settings. These platforms are also sufficiently robust that they allow repeated cycles of integration and removal from the skin, without damage to the electronics. The results in Figures S2a and S2b show examples of such use with both Tegaderm and silicone tape, respectively. With spray-on-bandage applied to the boundaries of the Tegaderm, robust integration with the skin is possible for as long as 2 weeks (Figure S2a). Properties of several candidate materials, including modulus, thickness, adhesive force, contact angle, and chemical composition are summarized in Table 1.

EES for sensing demonstrations use an FS layout (FS structures with 10 μm widths) to optimize contact with the skin, consistent with results shown in Figure 2. Finite element analysis of the mechanics shows the weak points of the serpentine structures upon uniaxial mechanical stretching in x- and y-directions (Figure 3b). Even though the serpentine traces experience more than 1% of maximum principle strains with 30% stretching, there were no observed mechanical fractures on the devices on

Table 1. Properties of several candidate materials.

	Silicone membrane (Ecoflex)	Silicone membrane (Solaris)	Spray-on-bandage	Tegaderm Film (3M)	Silicone Tape (3M)
Modulus [Pa]	-69×10^3	-172×10^3	-85×10^6	-12×10^6	-127×10^6
Thickness [μm]	~ 20	~ 20	~ 1	~ 35	~ 330
Adhesive force ^{a,b} [N]	0.24 ± 0.02	0.37 ± 0.01	0.98 ± 0.03	1.02 ± 0.01	1.37 ± 0.01
Contact angle ^b [$^\circ$]	110.1 ± 0.3	124.1 ± 0.9	92.9 ± 0.3	94.4 ± 0.5	104.4 ± 0.3
Chemical ingredient	Silicone elastomer	Silicone elastomer	Acrylate terpolymer, Polyphenylm-ethylsiloxane, Hexamethyldisiloxane	Acrylate polymer, Polyurethane, Polyester, Silicone film	Silicone adhesive, Acrylate polymer, Thermoplastic polyester

^a) The force was measured on a square sheet with an area of 9 cm^2 ; ^b) Error bar shows standard deviation (number of trials = 3).

skins. This mechanics, combined with conformal coverage on the skin, enables precision measurements, particularly for the case of EP where direct contact is critically important.

Comparisons of the electrical impedance of EES and conventional gel-based metal electrodes (E21-9 disk, Electro-cap international, USA) involve a pre-amplifier (James Long Co., USA) and sinusoidal inputs with frequency and amplitude of 37 Hz and $0.5 V_{\text{rms}}$ (root-mean-square voltage), respectively. In all cases, the tests use three electrodes (MEA, GND, and REF), each within a square area of 1 cm^2 and spaced by $\sim 1.8 \text{ cm}$ (center-to-center) for both of the EES and conventional electrodes. As shown in Figures S2c and S2e, $10 \mu\text{m}$ FS electrodes with this design (which, by consequence of the FS mesh design, involve only $\sim 20\%$ areal contact, Figure S2g) show impedances, of $\sim 35 \text{ k}\Omega$. Conventional circular electrodes with 1 cm diameter show impedances of $\sim 40 \text{ k}\Omega$ and $\sim 180 \text{ k}\Omega$, with and without the use of conductive gels, respectively (see illustrations in Figures S2d and S2f).

A commercial wireless data acquisition system (DAQ; Bio-Radio 150, Cleveland Medical Devices, USA; 2.4 GHz RF band, 100 ft light-of-sight transmission range) provides a convenient means to record EP signals detected with EES. The experimental setup includes an EES, a wireless transmitter, a USB-type receiver, and a laptop computer with data recording software (Figure S3a). To allow periodic measurements during long term wearability tests, we use releasable connectors that incorporate FS type designs and low modulus, silicone substrates ($500 \mu\text{m}$ -thick; Solaris, Smooth-On). The excellent mechanical compliance of these connectors enables reversible, low resistance electrical contacts through the action of van der Waals adhesion forces alone (Figures 3c and 3d). The connector includes seven separate pads for EP, temperature, and strain sensors (schematic and stretching photo in Figures S3b and S3c, respectively). An example of long-term health monitoring involves EES based recording of surface electromyography (EMG) and electrocardiography (ECG) signals at various times during the course of a week. Here, the GND electrode, located between the MEA and REF electrodes ($\sim 3.6 \text{ cm}$ apart at center-to-center distance), defines the common zero potential. The EP signal corresponds to the potential difference between the MEA and REF electrodes. Measured signals transmit wirelessly to the receiver; analysis uses commercial software with 60 Hz notch and high-pass Butterworth filters (BioRadio 150, Cleveland Medical Devices, USA). The surface EMG corresponds to

signal measured on the forearm during bending of the wrist every 30 seconds periodically. Figure 3e shows representative data collected shortly after mounting the EES. The behaviors include expected high frequency oscillations with amplitudes between $500 \mu\text{V}$ to 1 mV . Similar EMG measurements performed with the same device after one week are similar, although with slightly increased noise, possibly due to accumulated dead cells on the surface of the skin surface. In both cases, the signal-to-noise ratios compare favorably to those obtained using freshly applied conventional electrodes with conductive gels (Figure S3d). We note that after removal of the EES and spray-on-bandage with Scotch tape, the skin surface shows no adverse effects or allergic reactions (Figures S3e and S3f).

Operation of the EES strain sensor is illustrated through responses to cyclical bending of a wrist. The induced strains change the resistance of the Si NM, which is detected and recorded with 60 Hz notch and low-pass (Butterworth) filters. Figure 3f shows typical data. The gauge factor (GF) is defined by

$$GF = (\Delta R/R_0)/\epsilon \quad (1)$$

where ΔR is the resistance change, R_0 is the initial state, and ϵ is the strain deformation. Although the GF of single crystalline silicon itself is ~ 100 , the effective GF of the Si NM resistor when implemented in the FS EES layout is ~ 5 under uniaxial in-plane strain (Figure S3g). This difference is expected, and results from the configuration of the sensor and the FS mesh. Figure 3g presents recordings of temperature change on the forearm using a sensor that has a sensitivity of $1.43 \Omega \text{ } ^\circ\text{C}^{-1}$ (Figure S3h), separately calibrated with an infrared thermometer (Kintrex, USA). As a demonstration, the temperature sensor can detect the change of skin surface temperature caused by exposure to warm air from a hair dryer. The presented data show the resistance change recorded 5 seconds after the removal of hot air (red bar in the graph). The results indicate an increase in temperature of $\sim 1.8 \text{ } ^\circ\text{C}$. In another case, the sensor reveals temperature changes induced by running in place (blue bar in the graph). After running for 30 seconds, and then standing at rest for 5 seconds, the measured temperature change is $\sim 3.2 \text{ } ^\circ\text{C}$. Figure 3h shows, as an example of the multi-functional capabilities, ECG signals and breathing patterns simultaneously monitored using an EES mounted on the chest. Here, the strain sensor measures the movement of the chest associated with breathing. The graph of Figure 3i illustrates the

relative resistance change $((R - R_0)/R_0)$, where R_0 is the undeformed resistance, and R is the measured value) over a span of 60 seconds. The same EES enables measurement of ECG signals at various times over a period of seven days (Figure 3j with notch and Butterworth low-pass filters).

In summary, advanced materials and integration schemes yield improved mechanics and robustness of bonding in EES designed for monitoring of body responses through and on the skin. Biocompatible, spray-on acrylate/silicone bandage materials serve as both adhesives and encapsulants. EES with narrow FS mesh designs provide a basis for conformal contact, even in the roughest regions of the skin, in ways that simultaneously enable high performance monitoring. Microscopy studies show the extremely conformable nature of contact between 10 μm wide FS traces and the skin. Surgical tapes enable removal and re-use of such devices. Future work focuses on expanded classes of sensors, as well as devices for wireless power supply and communication. Advanced materials development will continue to play a key role in progress.

Experimental Section

Fabrication of a multifunctional epidermal electronics in a printable format: The fabrication began with high temperature diffusion doping of Si NMs (260 nm in thickness) on a silicon-on-insulator wafer (SOI, p-type, SOITEC, France). The doped NMs were patterned into the form of parallel arrays of ribbons, released from the wafer by etching the buried oxide with hydrofluoric acid and then transfer printing onto a layer of polyimide (PI; 0.3 μm in thickness through dilution with pyrrolidinone, Sigma-Aldrich, USA) coated on a temporary handle substrate (Si wafer, 4 inches in diameter, 475–575 μm in thickness, WRS materials, USA). The remaining fabrication processes involved conventional microfabrication techniques. In particular, photolithography and dry etching defined 'dog-bone' shaped structures from the transferred Si NMs to yield the active components for piezoresistive strain sensors. Photolithographically defined meander traces of Ti/Pt (5/40 nm in thickness) deposited by sputtering formed the temperature sensors. EP sensors used patterns of Cr/Au (5/200 nm in thickness) defined by photolithography and wet etching of metal deposited by electron beam evaporation. The total thickness of the multifunctional sensor system was only $\sim 0.8 \mu\text{m}$, in its thickest region. The top and bottom layers of PI (each 0.3 μm thick) placed the active sensing components in the neutral mechanical plane (NMP). By necessity, the Au for the EP sensors was outside of the NMP, to allow direct contact with the skin. For data acquisition, electrical contact pads were exposed by dry etching the top PI layer after removing the device from the handle substrate with a water soluble tape. The exposed pads allowed electrical connection to a releasable connector, by simple physical contact.

Measurement of adhesion force: The strength of adhesion between various materials and the skin was determined by measuring the force required to induce peeling, with a digital force meter (Mark-10, USA). The measurement location was the inner surface of the left forearm, shaved to remove any hair and then cleaned with a pad soaked in alcohol. In all cases, the test coupon consisted of a thin, square sheet with a fixed area (9 cm^2). The measurement protocol (Figure S3i) involved strapping the forearm in a fixed position, with the test coupon connected to the force meter. The peeling was conducted at room temperature, in an upward direction, against gravity, with a maximum speed (1000 mm min^{-1}). The peeling speeds were selected to lie in a range defined by a previous report.^[16] The adhesion force corresponds to the maximum value recorded just prior to complete removal of the coupon from the skin. These procedures are similar to those presented in previous studies of adhesion in medical dressings.^[16]

Experiments on human subjects: All experiments on human skins were conducted under approval from Institutional Review Board at the University of Illinois at Urbana-Champaign (protocol number: 13229). There are six subjects (age: 21–32, all males), co-authors in the paper. Research was carried out with informed signed consents from the subjects.

Supporting Information

Supporting Information is available from the Wiley Online Library or from the author.

Acknowledgements

W.H.Y. and Y.K. contributed equally to this work. We thank Woosik Lee and Sungyoung Jung for help with material preparation and data analysis. This study is supported by the National Science Foundation under Grant DMI-0328162 and the US Department of Energy, Division of Materials Sciences under Award No. DE-FG02-07ER46471 through the Materials Research Laboratory and Center for Microanalysis of Materials (DE-FG02-07ER46453) at the University of Illinois at Urbana-Champaign. J.A.R. acknowledges a National Security Science and Engineering Faculty Fellowship.

Received: October 24, 2012

Revised: January 8, 2013

Published online: February 26, 2013

- [1] J. Y. Baek, J. H. An, J. M. Choi, K. S. Park, S. H. Lee, *Sensor Actuat. a-Phys.* **2008**, *143*, 423.
- [2] H. C. Jung, J. H. Moon, D. H. Baek, J. H. Lee, Y. Y. Choi, J. S. Hong, S. H. Lee, *IEEE T. Bio-Med. Eng.* **2012**, *59*, 1472.
- [3] M. K. Kwak, H. E. Jeong, K. Y. Suh, *Adv. Mater.* **2011**, *23*, 3949.
- [4] C. T. Lin, L. D. Liao, Y. H. Liu, I. J. Wang, B. S. Lin, J. Y. Chang, *IEEE T. Bio-Med. Eng.* **2011**, *58*, 1200.
- [5] A. Searle, L. Kirkup, *Physiol. Meas.* **2000**, *21*, 271.
- [6] G. Ruffini, S. Dunne, L. Fuentesmilla, C. Grau, E. Farres, J. Marco-Pallares, P. C. P. Watts, S. R. P. Silva, *Sensor Actuat. a-Phys.* **2008**, *144*, 275.
- [7] D. H. Kim, N. S. Lu, R. Ma, Y. S. Kim, R. H. Kim, S. D. Wang, J. Wu, S. M. Won, H. Tao, A. Islam, K. J. Yu, T. I. Kim, R. Chowdhury, M. Ying, L. Xu, M. Li, H. J. Chung, H. Keum, M. McCormick, P. Liu, Y. W. Zhang, F. G. Omenetto, Y. G. Huang, T. Coleman, J. A. Rogers, *Science* **2011**, *333*, 838.
- [8] Y. Takema, Y. Yorimoto, M. Kawai, G. Imokawa, *Brit. J. Dermatol.* **1994**, *131*, 641.
- [9] Y. Barrandon, H. Green, *Proc. Natl. Acad. Sci. USA* **1985**, *82*, 5390.
- [10] L. Tchivaleva, H. Zeng, I. Markhvida, M. D. H. Lui, T. Lee, in *Skin Roughness Assessment (New Developments in Biomedical Engineering)*, D. Campolo, Ed. (InTech, www.intechopen.com/download/pdf/pdfs_id/9090, **2010**).
- [11] K. P. Wilhelm, P. Elsner, E. Berardesca, *Bioengineering of the Skin: Skin Surface Imaging and Analysis*. CRC: Boca Raton, **1997**.
- [12] R. D. Benfield, E. R. Newton, T. Hortobagyi, *Biol. Res. Nurs.* **2007**, *8*, 195.
- [13] S. J. Choi, J. H. Lee, Y. H. Lee, D. Y. Hwang, H. D. Kim, *J. Appl. Polym. Sci.* **2011**, *121*, 3516.
- [14] W. M. Silvers, D. G. Dolny, *J. Electromyogr. Kinesiol.* **2011**, *21*, 95.
- [15] Z. Zhang, A. Conway, A. B. Salamone, E. T. Crumpler, X. Zhang, C. Z. Li, *Front. Biosci.* **2010**, *2*, 1123.
- [16] J. Klode, L. Schottler, I. Stoffels, A. Korber, D. Schadendorf, J. Dissemond, *J. Eur. Acad. Dermatol.* **2011**, *25*, 933.